

Faculty of Engineering
Faculty of Engineering - Papers

University of Wollongong

Year 2006

Transport properties of multilayered
MgB₂/Mg₂Si superconducting thin film

Y. Zhao* M. J. Qin[†] S. X. Dou[‡]
M. Ionescu** P. Munroe^{††}

*University of Wollongong

[†]University of Wollongong, qin@uow.edu.au

[‡]University of Wollongong, shi@uow.edu.au

**ANSTO, Australia

^{††}University of New South Wales

This article was originally published as: Zhao, Y, Qin, MJ, Dou, SX, Ionescu, M & Munroe, P, Transport properties of multilayered MgB₂/Mg₂Si superconducting thin film, Journal of Applied Physics, April 2006, 99, 08M503. Copyright American Institute of Physics. Original journal available here.

This paper is posted at Research Online.

<http://ro.uow.edu.au/engpapers/159>

Transport properties of multilayered $\text{MgB}_2/\text{Mg}_2\text{Si}$ superconducting thin film

Y. Zhao,^{a)} M. J. Qin, and S. X. Dou

Institute for Superconducting and Electronic Materials, University of Wollongong, Wollongong, New South Wales 2522, Australia

M. Ionescu

Australian Nuclear Science and Technology Organization (ANSTO), Menai, New South Wales 2234, Australia

P. Munroe

Electron Microscope Unit, University of New South Wales, Sydney, New South Wales 2052, Australia

(Presented on 2 November 2005; published online 25 April 2006)

Electronic transport measurements have been carried out on superconducting $\text{MgB}_2/\text{Mg}_2\text{Si}$ multilayer film, using a standard four-probe method in perpendicular and parallel applied fields. The film, which was prepared by pulsed-laser deposition, has a layered structure with each MgB_2 layer being 40–50 nm thick and the Mg_2Si interlayers about 5 nm thick. The flux flow activation energy is deduced from the resistivity-temperature curves using an Arrhenius fit. The results show a clearly enhanced anisotropy of the vortex activation energy in the multilayered film. The irreversibility field and the vortex activation energy are significantly increased in parallel fields. © 2006 American Institute of Physics. [DOI: [10.1063/1.2172558](https://doi.org/10.1063/1.2172558)]

Inherent or artificially introduced layered structure is an interesting topic for superconductors. There have been a number of experimental reports on multilayered low temperature superconductors^{1–4} and high temperature superconductors (HTSs).^{5–8} A layered superconductor usually shows different behaviors from that of the bulk, such as the crossover from three dimensional to two dimensional upper critical field (H_{c2}) behavior,^{2,9,10} the scaling effect in the angular dependence of critical current density (J_c),¹¹ and enhanced anisotropy in the vortex pinning energy.¹² These phenomena can be a good tool in revealing the pinning mechanism and superconducting parameters for the superconductors. Lawrence and Doniach have proposed a weak Josephson coupling model for superconductor/insulator superlattices.¹³ The model was then extensively studied by Klemm *et al.*⁹ and extended into superconductor/normal conductor superlattices by Takahashi and Tachiki.¹⁰ The model explains successfully the temperature dependence of the upper critical field of the superconducting superlattices and intrinsically layered HTSs.

The moderate temperature superconductor MgB_2 has a layered structure and two separate superconducting gaps.^{14,15} The Ginzburg-Landau (GL) coherence length $\xi(0)$ is about 10 nm within the a - b plane and 5 nm along the c axis for MgB_2 .¹⁶ Because the coupling between the B layers in MgB_2 ($c=0.352$ nm) is strong, the superconductor does not display the intrinsic two dimensional pancake vortices that have been observed in HTSs.¹⁷

Mg_2Si is a very stable semiconductor and can be easily formed from Mg+Si at a temperature as low as 200° C. By sequentially switching the MgB_2 and Si targets during an off-axis pulsed laser deposition (PLD) process, we have successfully obtained a $\text{MgB}_2/\text{Mg}_2\text{Si}$ multilayer structure in the

thin film with an undamaged T_c . In this paper we report transport measurements on the $\text{MgB}_2/\text{Mg}_2\text{Si}$ multilayer film using a standard four-probe method.

In the PLD process, a stoichiometric MgB_2 target (84% density), a Si target, and a magnesium target were set on a carousel in the chamber. The laser beam was generated by an excimer laser system (Lambda-Physik) operating on KrF gas ($\lambda=248$ nm, 25 ns). The chamber was first evacuated to a base vacuum of about 8×10^{-8} Torr and then filled with high purity argon to 120 mTorr as the background gas. Before the deposition, the heater was kept at 250 °C. Sapphire c -cut substrates with dimensions of about 6×2 mm² were used. With an off-axis geometry,¹⁸ the substrate is parallel to the normal axis of the target surface and aligned to the center of the laser spot. The substrate is mounted onto the edge of the heater with silver paste. We switched the MgB_2 and Si targets ten times during the deposition. At the end of the deposition, the Mg target was switched to the depositing position to provide a protective Mg cap layer. Then the Ar pressure was increased to 760 Torr before the *in situ* annealing. The films were heated to 650 °C in 12 min and kept at that temperature for 1 min. For comparison, monolayer MgB_2 films were prepared under the same conditions and are referred to as MgB_2 film in the following text. The resulting films have a thickness of 400–500 nm, as detected by atomic force microscopy (AFM) and transmission electron microscopy (TEM). The TEM works were done on a JEM-200 (JEOL) working at 200 kV. The cross-sectional TEM specimen was prepared with a focused ion beam using a Ga source.

The transport measurements were carried out using a four-probe method with a dc current density of 10 A/cm². In both the $H \parallel ab$ -plane (parallel field) and $H \perp ab$ -plane (perpendicular field) cases, the testing current was perpendicular to the applied field.

Figure 1 is a cross-sectional scanning electron micros-

^{a)}Electronic mail: yz70@uow.edu.au

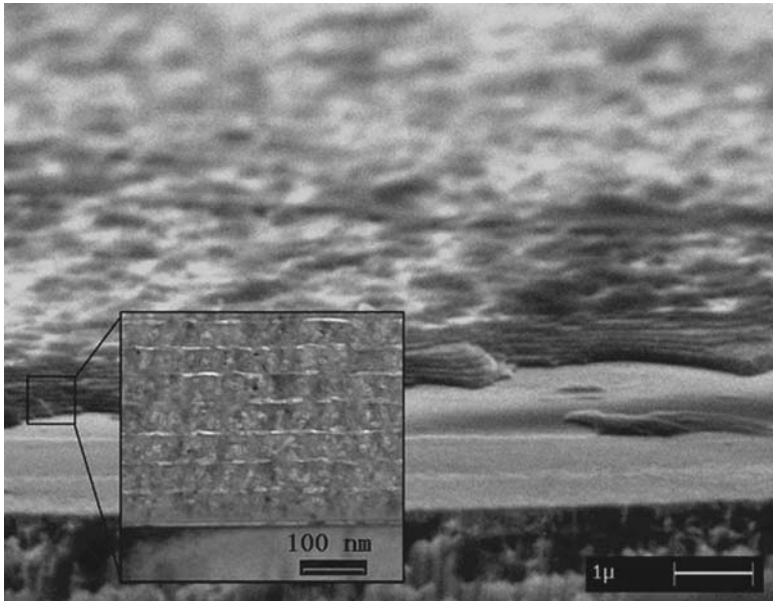


FIG. 1. Cross-sectional SEM image of the multilayer film. The inset is a TEM BF image of the multilayer film.

copy (SEM) image of the Si-added MgB_2 film. It shows a multilayer structure within the film. A TEM bright field (BF) image is shown in the inset of Fig. 1, illustrating that the MgB_2 layers are 40–50 nm thick and the interlayers are about 5 nm thick. Each MgB_2 layer consists of very fine grains. Individual grains are less than 20 nm in size. The 5 nm thick interlayers between the ten MgB_2 layers are Mg_2Si , judging from the electron diffraction and x-ray energy dispersive spectroscopy (EDS) results. The existence of Mg_2Si is in accordance with previous reports on Si addition in the Mg-B system.^{19,20}

The zero resistivity T_c of the multilayer film is 31 K, slightly suppressed by ~ 1.5 K compared with the MgB_2 film. The transition widths from 10% $\rho(40\text{ K})$ to 90% $\rho(40\text{ K})$ for both films are the same, about 0.5 K in zero field. The narrow transition width of the multilayered film indicates that the MgB_2 phase remains homogeneous after the addition of Mg_2Si interlayers.

Figure 2 shows the field dependence of the resistivity-

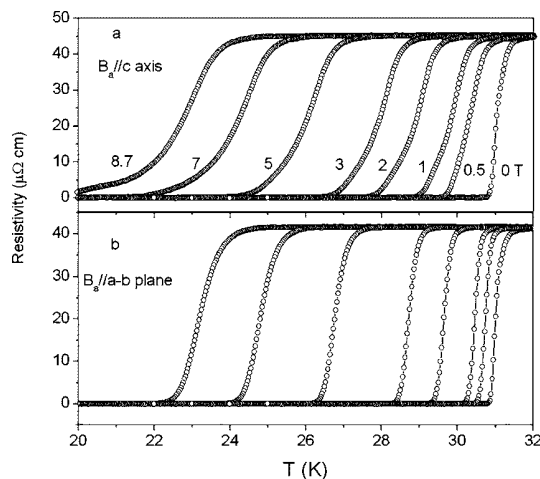


FIG. 2. Resistivity vs temperature curves of multilayer film in parallel and perpendicular fields. (a) In perpendicular fields and (b) in parallel fields.

temperature curves of the multilayer film in parallel and perpendicular applied field circumstances. The T_c 's are not shifted to lower temperatures as much in the parallel field condition, as with the perpendicular field condition. The T_c transition width is also narrower in parallel applied fields, indicating better pinning in the fields.

The irreversibility fields of the multilayer film and the MgB_2 film were derived from the transport curves using the 10% ρ_T^c values and are shown in Fig. 3. The irreversibility field H_{irr}^c for the multilayer film is almost identical to the H_{irr}^{ab} and H_{irr}^c of the MgB_2 film, showing the same level of flux pinning in the three circumstances. However, the H_{irr}^{ab} of the multilayer film has clearly increased, indicating a significant enhancement of pinning in parallel fields.

Although the activation energy of the thermally assisted flux flow (TAFF) for MgB_2 is significantly higher than that of HTS, TAFF is still detectable through the resistivity-temperature curves for different applied fields.^{21,22} The activation energy U_0 of our MgB_2 and multilayer films is estimated from the Arrhenius law,^{22–24} $\rho = \rho_0 \exp(-U_0/k_B T)$, where ρ_0 is a field-independent preexponential factor and k_B is Boltzmann's constant. The Arrhenius plots of resistance

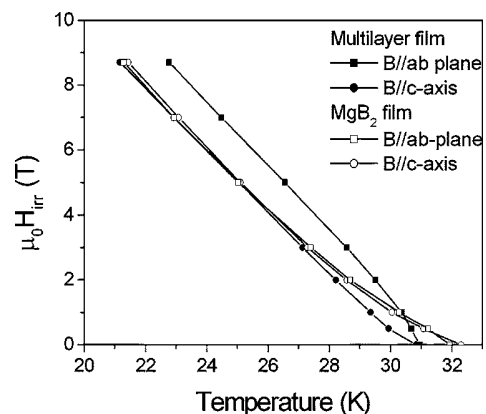


FIG. 3. The irreversibility fields of the multilayer film and the MgB_2 film.

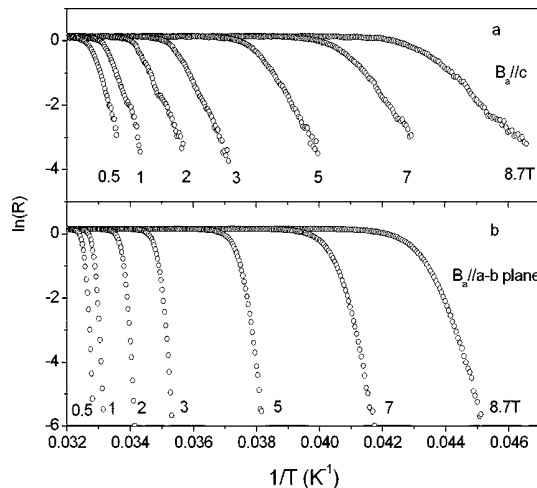


FIG. 4. The Arrhenius plot of resistance $R(T, H)$ for the multilayer film in (a) perpendicular and (b) parallel fields.

$R(T, H)$ for the multilayer film in perpendicular and parallel fields are shown in Fig. 4. In both perpendicular [Fig. 4(a)] and parallel fields [Fig. 4(b)], there is clearly a linear part in each $\ln(R) - 1/T$ curve which represents the TAFF regime in the multilayered film. A similar linear dependence of $\ln(R)$ on $1/T$ is also observed in our MgB_2 films.

Figure 5 shows the activation energy of the flux flow versus applied field B_a . The activation energy of the MgB_2 film is 0.6–0.7 eV in the low field regime for both perpendicular and parallel fields. The depression of anisotropy in our c -oriented monolayer film could be a consequence of the strong scattering found in the films.¹⁸ U_0 is significantly increased in the multilayer film (about 2 eV in the low field regime) when the applied field is parallel to the a - b plane of the film, but in perpendicular fields U_0 is considerably suppressed.

The introduced anisotropy of U_0 and H_{irr} can be well explained within GL theory for layered superconductors. The thickness of the nonsuperconducting Mg_2Si interlayer is typically 5 nm, of the same order as $\xi_{ab}(0)$ of MgB_2 . The coupling of vortices across the Mg_2Si layer is relatively weak. When the applied field is parallel to the a - b plane, the vortices are probably trapped in the nonsuperconducting

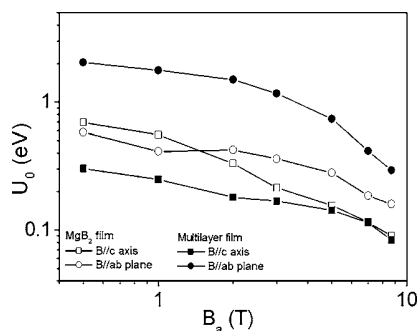


FIG. 5. The activation energy U_0 of flux flow vs applied field B_a .

Mg_2Si layers. Thus the two dimensional Mg_2Si defect both provides strong flux pinning and increases the thermal activation energy for flux flow in the parallel field. The activation energy for the multilayer film is decreased in perpendicular fields compared with the MgB_2 film, which may imply an easier TAFF due to the vortex decoupling across the nonsuperconducting interlayers, a phenomenon that has been observed and studied in HTS and other artificially multilayered superconducting films.^{5,12}

To conclude, strong differences in transport properties are introduced by artificially introduced multilayer structure in $\text{MgB}_2/\text{Mg}_2\text{Si}$ thin films. Much better pinning is observed in parallel fields, judging from the $\rho(T, H)$ curves. The activation energy U_0 is significantly increased when the applied field is perpendicular to the c axis which is in accordance with the enhancement of H_{irr}^{ab} . However, in perpendicular fields, the U_0 is dramatically lower, which may be due to weakened vortex coupling across the 5 nm thick nonsuperconducting interlayer.

This work was supported by the Australian Research Council, Hyper Tech Research Inc., OH, USA, Alphatech International Ltd., NZ, and the University of Wollongong.

- ¹S. T. Ruggiero, T. W. Barbee, Jr., and M. R. Beasley, Phys. Rev. Lett. **45**, 1299 (1980).
- ²M. G. Karkut, V. Matijasevic, L. Antognazza, J. M. Triscone, N. Missert, M. R. Beasley, and O. Fischer, Phys. Rev. Lett. **60**, 1751 (1988).
- ³J. M. Murduck, D. W. Capone II, I. K. Schuller, S. Foner, and J. B. Ketterson, Appl. Phys. Lett. **52**, 504 (1988).
- ⁴I. K. Schuller, Phys. Rev. Lett. **44**, 1597 (1980).
- ⁵J. L. Martin, M. Velez, and J. L. Vicent, Phys. Rev. B **52**, R3872 (1995).
- ⁶K.-H. Kim, H.-J. Kim, S.-I. Lee, A. Iyo, Y. Tanaka, K. Tokiwa, and T. Watanabe, Phys. Rev. B **70**, 092501 (2004).
- ⁷P. N. Barnes, T. J. Haugan, C. V. Varanasi, and T. A. Campbell, Appl. Phys. Lett. **85**, 4088 (2004).
- ⁸J. Hanisch, C. Cai, R. Huhne, L. Schultz, and B. Holzapfel, Appl. Phys. Lett. **86**, 122508 (2005).
- ⁹R. A. Klemm, A. Luther, and M. R. Beasley, Phys. Rev. B **12**, 877 (1975).
- ¹⁰S. Takahashi and M. Tachiki, Phys. Rev. B **33**, 4620 (1986).
- ¹¹G. Jakob, M. Schmitt, T. Kluge, C. Tomerose, P. Wagner, T. Hahn, and H. Adrian, Phys. Rev. B **47**, 12099 (1993).
- ¹²J. R. Clem, Supercond. Sci. Technol. **11**, 909 (1998).
- ¹³W. E. Lawrence and S. Doniach, in *Proceedings of the 12th International Conference on Low Temperature Physics*, Tokyo, 1971 (Academic Press of Japan, Kyoto, 1971), p. 361.
- ¹⁴I. I. Mazin and V. P. Antropov, Physica C **385**, 49 (2003).
- ¹⁵H. J. Choi, M. L. Cohen, and S. G. Louie, Physica C **385**, 66 (2003).
- ¹⁶A. D. Caplin, Y. Bugoslavsky, L. F. Cohen, L. Cowey, J. Driscoll, J. Moore, and G. K. Perkins, Supercond. Sci. Technol. **16**, 176 (2003).
- ¹⁷J. R. Clem, Supercond. Sci. Technol. **5**, S33 (1992).
- ¹⁸Y. Zhao, M. Ionescu, J. Horvat, and S. X. Dou, Supercond. Sci. Technol. **18**, 395 (2005).
- ¹⁹X. L. Wang, S. H. Zhou, M. J. Qin, P. R. Munroe, S. Soltanian, H. K. Liu, and S. X. Dou, Physica C **385**, 461 (2003).
- ²⁰L. D. Cooley, K. Kang, R. Klie, Q. Li, A. Moodenbaugh, and R. Sabatini, Supercond. Sci. Technol. **17**, 942 (2004).
- ²¹S. Patnaik, A. Gurevich, S. D. Bu, S. D. Kaushik, J. Choi, C. B. Eom, and D. C. Larbalestier, Phys. Rev. B **70**, 064503 (2004).
- ²²A. Sidorenko, *et al.* cond-mat/0406062.
- ²³T. T. M. Palstra, B. Batlogg, R. B. von Dover, L. F. Schneemeyer, and J. V. Waszczak, Appl. Phys. Lett. **54**, 763 (1989).
- ²⁴T. T. M. Palstra, B. Batlogg, R. B. von Dover, L. F. Schneemeyer, and J. V. Waszczak, Phys. Rev. B **41**, 6621 (1990).